ELECTRONIC SUPPLEMENTARY INFORMATION (ESI)

Interesting chemical and physical features in the products of the reactions between trivalent lanthanoids and a tetradentate Schiff base derived from cyclohexane-1,2-diamine [+]

Ioannis Mylonas-Margaritis,*[a] Zoi G. Lada[b], Alexandros A. Kitos,[a] Diamantoula Maniaki,[a] Katerina Skordi,[c] Anastasios J. Tasiopoulos,[c] Vlasoula Bekiari,[d] Albert Escuer,[e] Julia Mayans,*[e] Vassilios Nastopoulos,*[a] Evangelos G. Bakalbassis,*[f] Dionissios Papaioannou*[a] and Spyros P. Perlepes*[a, b]

[a.] *Department of Chemistry, University of Patras, 26504 Patras, Greece. E-mail: ioanismylonasmargaritis@gmail.com; dapapaio@upatras.gr; nastopoulos@upatras.gr; perlepes@upatras.gr*
[b.] *Institute of Chemical Engineering Sciences (ICE-HT), Foundation for Research and Technology-Hellas (FORTH), P.O. Box 1414, Platani, 26504 Patras, Greece*
[c.] *Department of Chemistry, University of Cyprus, 1678 Nicosia, Cyprus*
[d.] *Department of Agriculture, University of Patras, 26504 Patras, Greece*
[e.] *Departament de Quimica Inorganica i Organica, Secio Inorganica and Institute of Nanoscience (IN2UB) and Nanotechnology, Universitat de Barcelona, Marti i Franques 1-11, 08028 Barcelona, Spain. E-mail: julia.mayans@qi.ub.edu*
[f.] *Department of Chemistry, Aristotle University of Thessaloniki, University Campus, 54124 Thessaloniki, Greece. E-mail: bakalbas@chem.auth.gr*

Table S1 Crystallographic data for compounds **1**, **3**, **5**, **6** and **8**

Parameter	**1**	**3**	**5**	**6**	**8**
Chemical formula	$C_{23}H_{32}PrN_5O_{12}$	$C_{23}H_{32}SmN_5O_{12}$	$C_{23}H_{32}GdN_5O_{12}$	$C_{23}H_{32}TbN_5O_{12}$	$C_{23}H_{32}HoN_5O_{12}$
M_r	711.44	720.88	727.78	729.45	735.46
Crystal size (mm)	0.18 x 0.15 x 0.12	0.19 x 0.15 x 0.11	0.16 x 0.15 x 0.11	0.17 x 0.15 x 0.10	0.15 x 0.14 x 0.10
Crystal system	Triclinic	Triclinic	Triclinic	Triclinic	Triclinic
Space group	$P\bar{1}$	$P\bar{1}$	$P\bar{1}$	$P\bar{1}$	$P\bar{1}$
a/Å	9.0693(5)	9.037(4)	9.0364(5)	9.0184(4)	9.0033(8)
b/Å	10.8628(4)	10.8222(6)	10.8141(5)	10.7887(4)	10.7752(10)
c/Å	15.4923(8)	15.4002(7)	15.3789(8)	15.3433(8)	15.3482(12)
α/°	72.376(4)	72.600(4)	72.768(4)	72.650(4)	72.575(8)
β/°	82.650(2)	82.703(4)	82.691(4)	82.897(4)	83.019(7)
γ/°	72.893(4)	73.013(4)	73.102(5)	73.220(4)	73.246(8)
V/Å^3	1389.01(12)	1373.63(12)	1372.01(13)	1363.11(11)	1359.3(2)
T/K	100(2)	100(2)	100(2)	100(2)	100(2)
Radiation/ μ (mm^{-1})	Mo Kα/ 1.83	Mo Kα/ 2.21	Mo Kα/ 2.49	Mo Kα/ 2.67	Cu Kα/ 6.08
No. of reflections measured	11755	11005	11951	10956	8963
No. of independent reflections (R_{int})	5995(0.035)	5937(0.035)	6070(0.037)	6042(0.032)	5147(0.032)
No. of observed reflections ($I>2\sigma(I)$)	5314	5324	5376	5537	4599
No. of restraints	2	2	2	3	3
R_1 [$F^2>2\sigma(F^2)$]	0.031	0.034	0.032	0.030	0.033
$wR_2(F^2)$	0.065	0.066	0.061	0.062	0.081
Goodness of fit on F^2	1.04	1.06	1.03	1.06	1.07
$\Delta\rho_{max}/\Delta\rho$ (e Å^{-3})	0.81, -0.54	1.27, -0.64	1.02, -0.69	1.38, -0.80	0.49, -0.80
CCDC number	2246268	2246270	2246269	2246271	2246267

Table S2 Geometry (Å, °) for the H bonds in the crystal structure of complex $[Pr(NO_3)_3(L'H_2)(MeOH)]$ (**1**)

H bond D-H···A[a,b]	D···A	H···A	D-H···A	Symmetry operation of A
N1-H1···O1	2.580(3)	1.78(3)	150(3)	
N2-H2···O2	2.594(3)	1.81(3)	148(3)	
O12-H12···O11	2.868(3)	2.05(3)	170(3)	-*x*+1, -*y*+1, -*z*+1
C3-H3···O7	3.357(4)	2.57	140	
C8-H8A···O10	3.334(4)	2.56	136	*x*, *y*+1, *z*
C8-H8C···O8	3.331(4)	2.43	152	*x*-1, *y*+1, *z*
C9-H9B···O8	3.453(4)	2.49	163	*x*-1, *y*+1, *z*
C6-H16C···O6	3.559(4)	2.64	157	-*x*+1, -*y*+1, -*z*
C19-H19···O6	3.280(4)	2.54	134	
C21-H21···O5	3.429(4)	2.66	139	-*x*+1, -*y*+1, -*z*

[a] Many of the involved non-H atoms have been numbered in Fig. 1.

[b] O5 is the "free" atom of the O3,O4-coordinated nitrato group, O8 is the "free" atom of the O6,O7-coordinated nitrato group, O11 is the "free" atom of the O9,O10-coordinated nitrato group, C8 and C16 are the carbon atoms of the methyl groups, C9 is the aliphatic carbon atom bonded to N1, while C19 and C21 are carbons of the aromatic ring which is connected to O2; these atoms have not been labelled in Fig. 1. D=donor; A= acceptor.

Table S3 Continuous Shape Measures (CShM) values for the potential coordination polyhedra of the Ln^{III} centre in the structures of the complexes $[Ln(NO_3)_3(L'H_2)(MeOH)]$ (Ln = Pr, **1**; Ln = Sm, **3**; Ln = Gd, **5**; Ln = Tb, **6**; Ln = Ho, **8**)[a]

Ideal coordination polyhedron	**1**	**3**	**5**	**6**	**8**
Enneagon	31.880	32.049	32.000	32.021	31.924
Octagonal pyramid	19.084	19.259	19.268	19.409	19.457
Heptagonal bipyramid	17.987	18.155	18.166	18.167	18.075
Johnson triangular cupola	13.930	13.955	13.901	13.920	13.818
Capped cube	11.307	11.181	11.125	11.060	11.147
Spherical-relaxed capped cube	10.391	10.385	10.336	10.311	10.239
Capped square antiprism	3.563	3.390	3.221	3.227	3.045
Spherical capped square antiprism	**2.733**	**2.560**	2.416	2.424	2.286
Tricapped trigonal prism	3.532	3.339	3.186	3.132	2.946
Spherical tricapped trigonal prism	3.001	2.973	2.867	2.829	2.715

[a] The polyhedron with the CshM value in bold is the real polyhedron of the Ln^{III} centre for each compound.

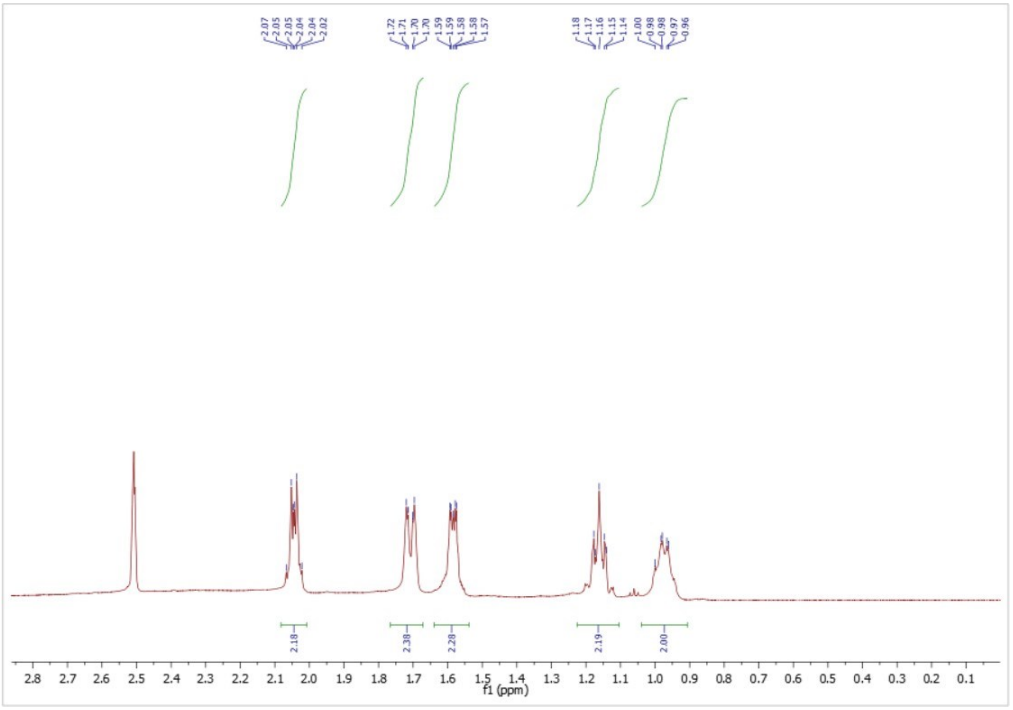

Fig. S1 The ^{1}H NMR spectrum (d_6-DMSO, δ/ppm) of (±)-*trans*-1,2-diaminocyclohexane used for the synthesis of LH_2 (Scheme 1). The signal at δ 2.52 ppm is due to the non-deuteriated portion of the solvent.

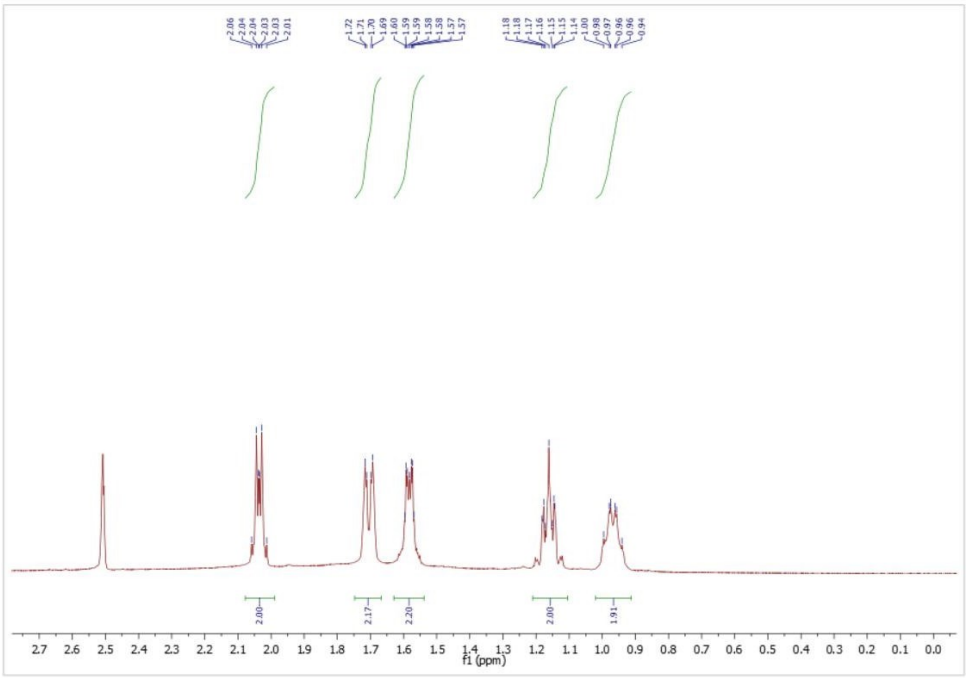

Fig. S2 The ^{1}H NMR spectrum (d_6-DMSO, δ/ppm) of (+)-*S*,*S*-*trans*-1,2-diaminocyclohexane provided by Fluorochem, CAS: 21436-03-3). The signal at δ 2.52 ppm is due to the non-deuteriated portion of the solvent.

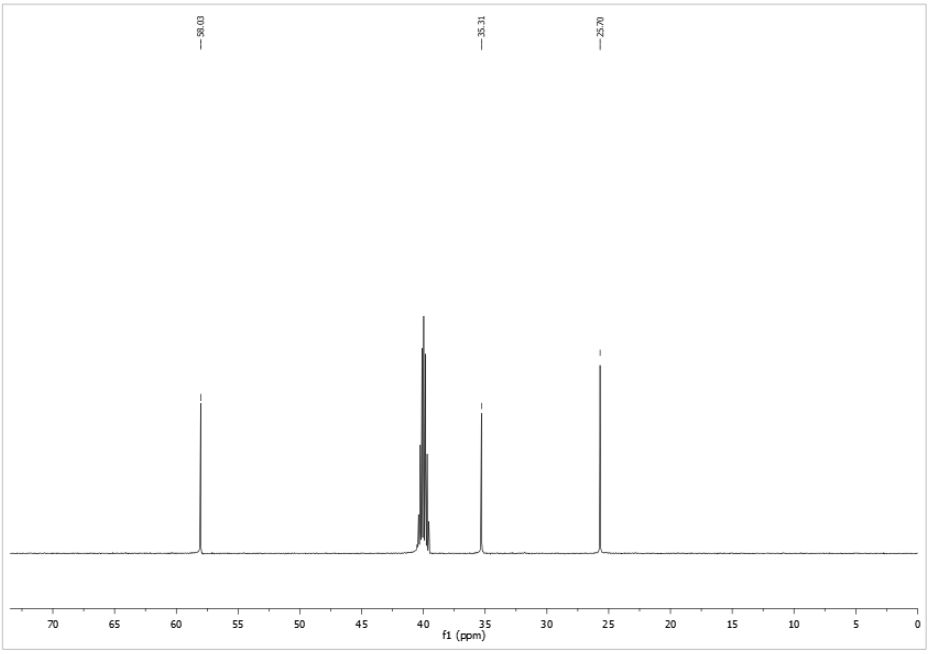

Fig. S3 The ^{13}C NMR spectrum (d_6-DMSO, δ/ppm) of (±)-*trans*-1,2-diaminocyclohexane used for the synthesis of LH_2 (Scheme 1). The signal at δ ~40 ppm is due to the carbon atoms of the solvent.

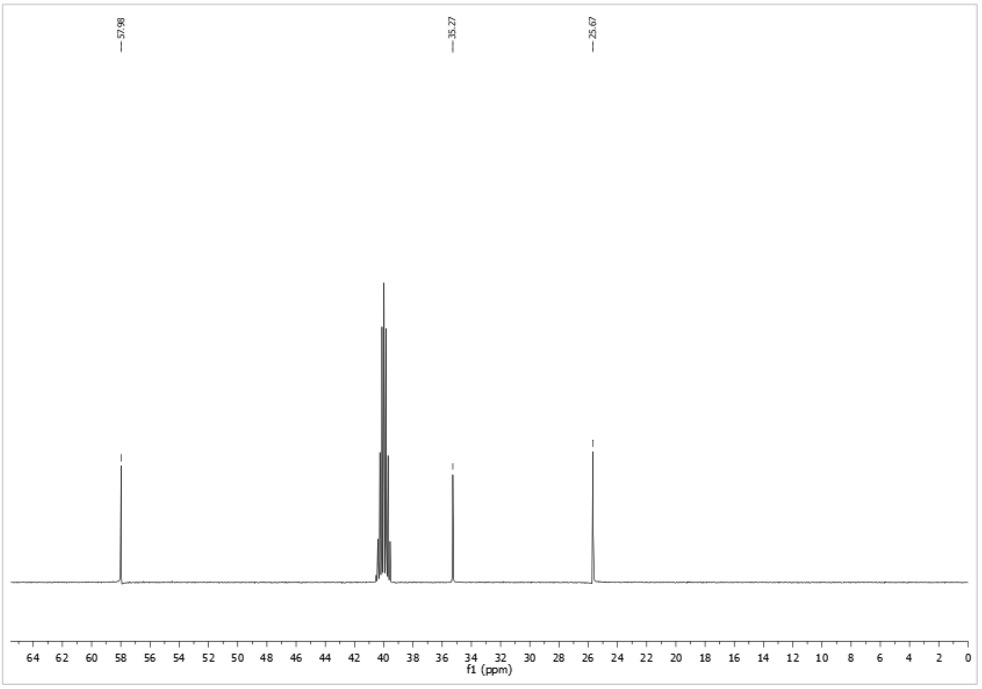

Fig. S4 The ^{13}C NMR spectrum (d_6-DMSO, δ/ppm) of (-)-*R*,*R*-*trans*-1,2-diaminocyclohexane provided by Fluorochem, CAS: 20439-47-8). The signal at δ ~40 ppm is due to the carbon atoms of the solvent.

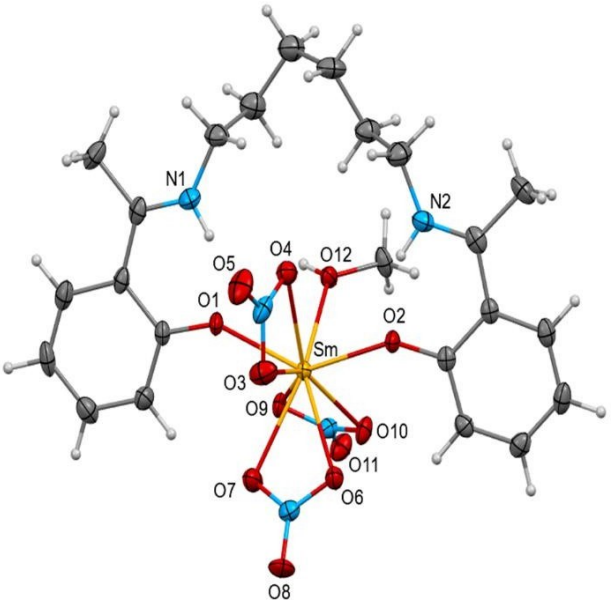

Fig. S5 Partially labelled plot of the structure of the molecule $[Sm(NO_3)_3(L'H_2)(MeOH)]$ that is present in complex **3**.Thermal ellipsoids are drawn at the 50% probability level. Selected bond lengths (Å): Sm-O1 2.295(2), Sm-O2 2.305(2), Sm-O12 2.451(2), Sm-O(nitrato) 2.481(3)-2.575(2).

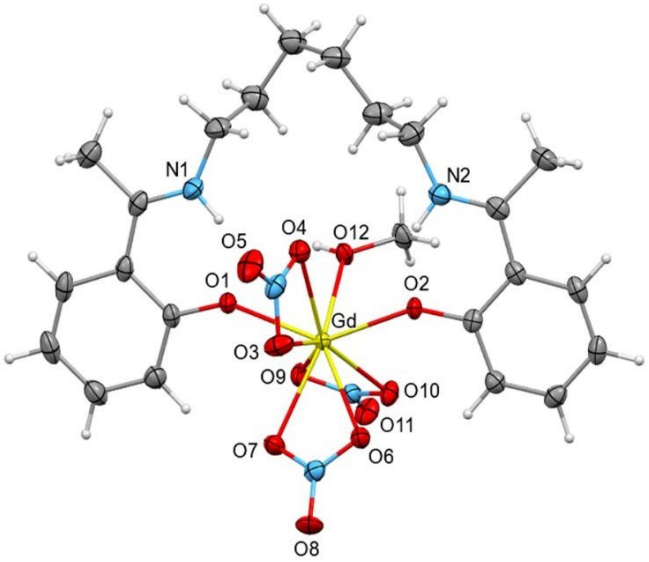

Fig. S6 Partially labelled plot of the structure of the molecule $[Gd(NO_3)_3(L'H_2)(MeOH)]$ that is present in complex **5**. Thermal ellipsoids are drawn at the 50% probability level. Selected bond lengths (Å): Gd-O1 2.284(2), Gd-O2 2.292(2), Gd-O12 2.423(2), Gd-O(nitrato) 2.453(2)-2.550(2).

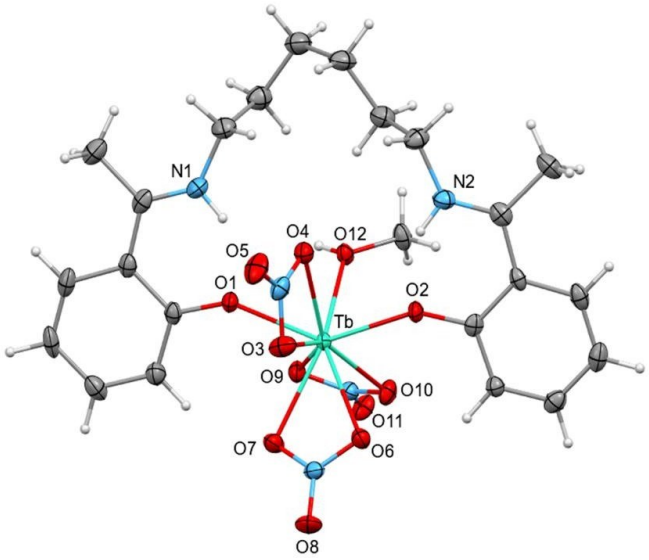

Fig. S7 Partially labelled plot of the structure of the molecule $[Tb(NO_3)_3(L'H_2)(MeOH)]$ that is present in complex **6**.Thermal ellipsoids are drawn at the 50% probability level. Selected bond lengths (Å): Tb-O1 2.260(2), Tb-O2 2.268(2), Tb-O12 2.409(2), Tb-O(nitrato) 2.442(2)-2.545(2).

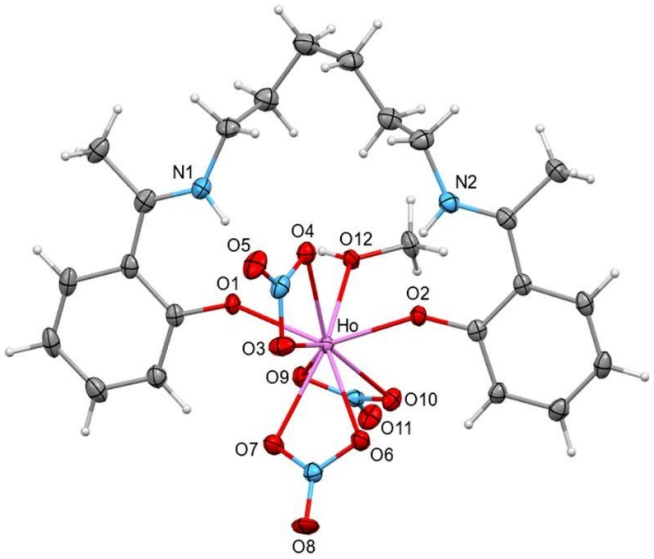

Fig. S8 Partially labelled plot of the structure of the molecule $[Ho(NO_3)_3(L'H_2)(MeOH)]$ that is present in complex **8**. Thermal ellipsoids are drawn at the 50% level. Selected bond lengths (Å): Ho-O1 2.251(2), Ho-O2 2.252(2), Ho-O12 2.391(2), Ho-O(nitrato) 2.414(2)-2.528(2).

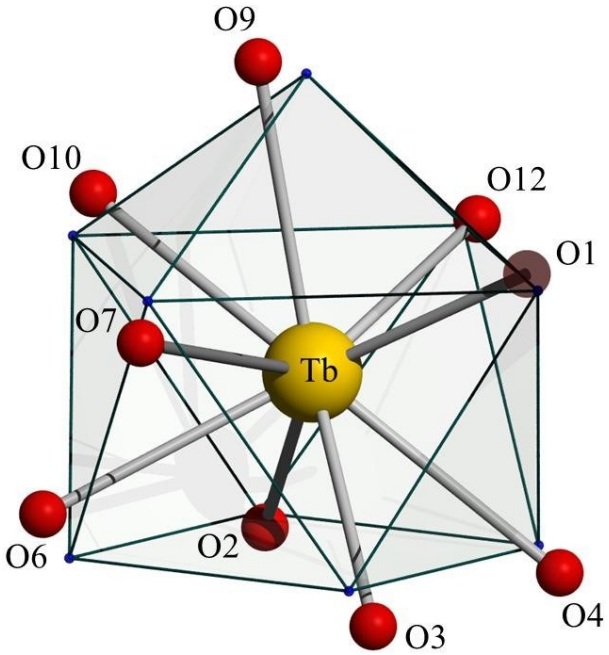

Fig. S9 The spherical capped square antiprismatic coordination polyhedron of Tb^{III} in complex **6**. The very small spheres define the vertices of the ideal polyhedron.

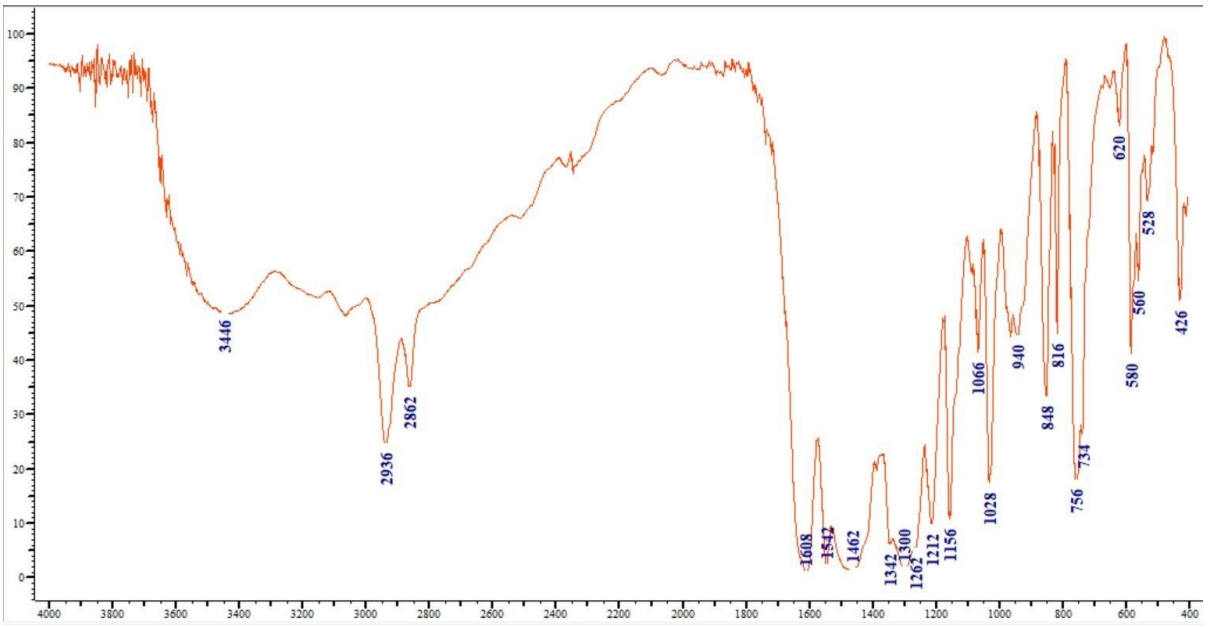

Fig. S10 The IR spectrum (KBr, cm^{-1}) of complex $[Pr(NO_3)_3(L'H_2)(MeOH)]$ (**1**).

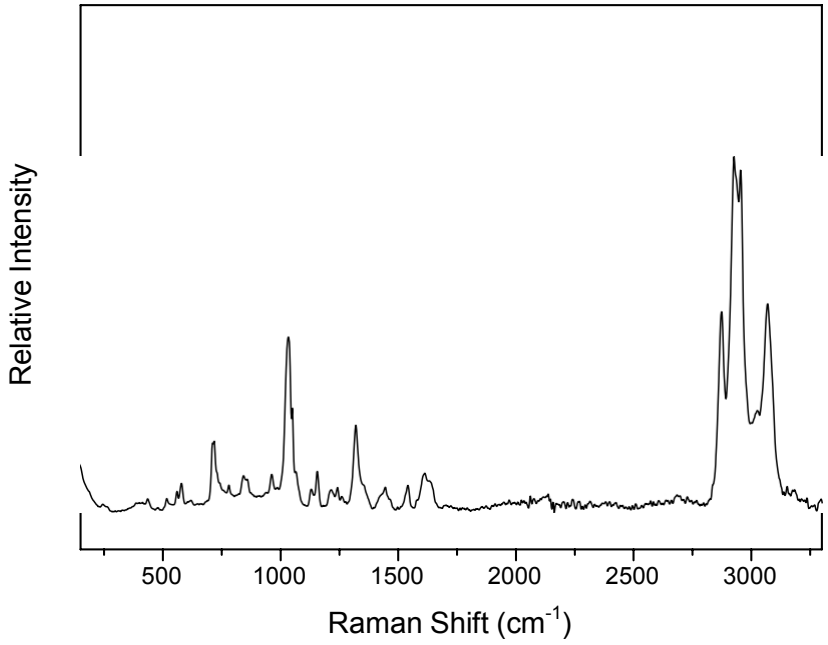

Fig. S11 The Raman spectrum of solid [Dy$(NO_3)_3$(L'H_2)(MeOH)] (**7**).

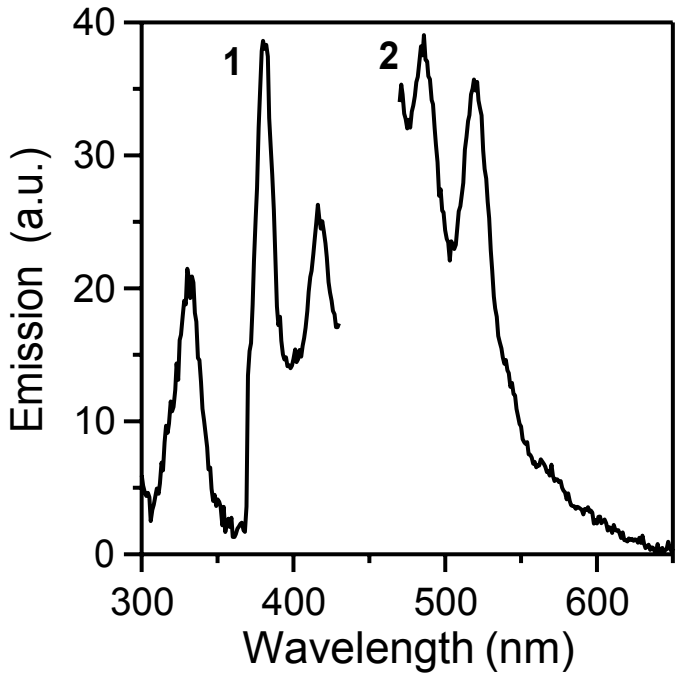

Fig. S12 Solid-state, room-temperature excitation (curve 1; maximum emission at 486 nm) and emission (curve 2; maximum excitation at 380 nm) spectra of solid [Dy$(NO_3)_3$(L'H_2)(MeOH)] (**7**).

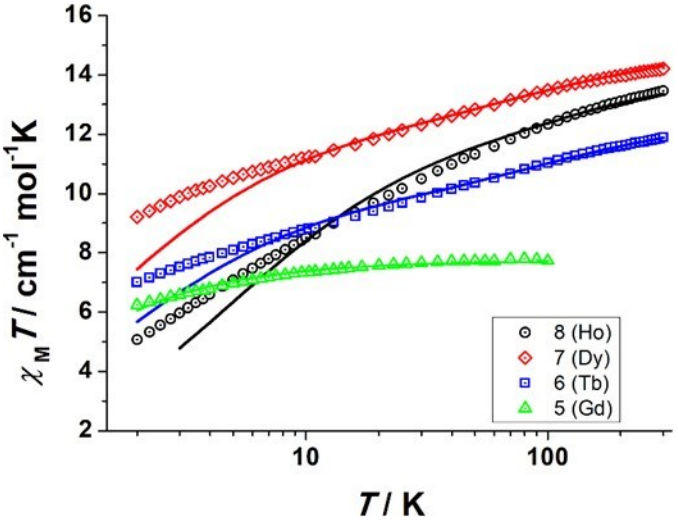

Fig. S13 Temperature dependence of the $\chi_M T$ product *vs*. log(*T*) for compounds **5** (triangles), **6** (squares), **7** (diamonds) and **8** (circles).

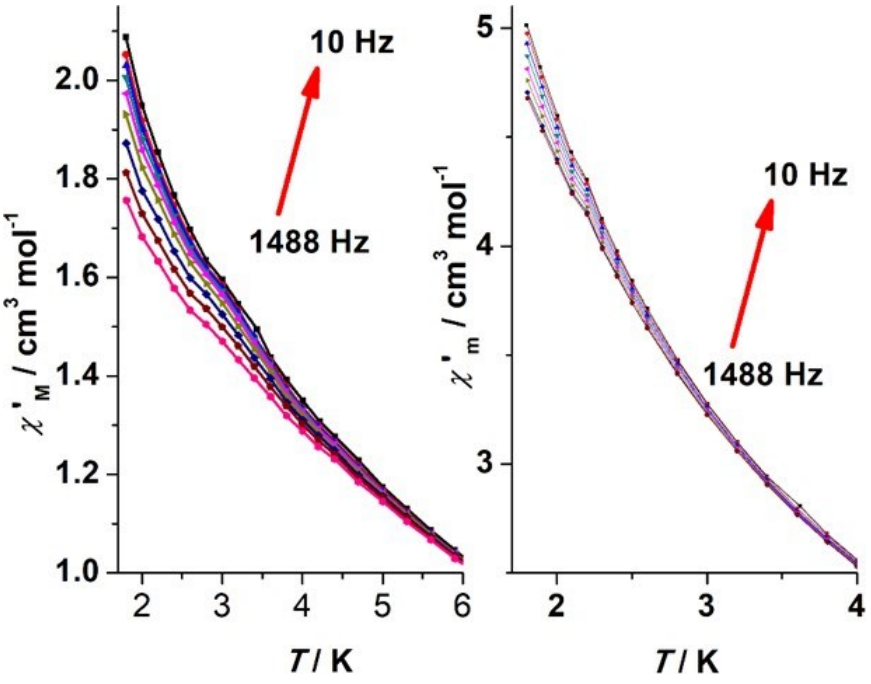

Fig. S14 In-phase magnetic susceptibility (χ_M') vs. *T* for complexes **5** (left) and **7** (right).

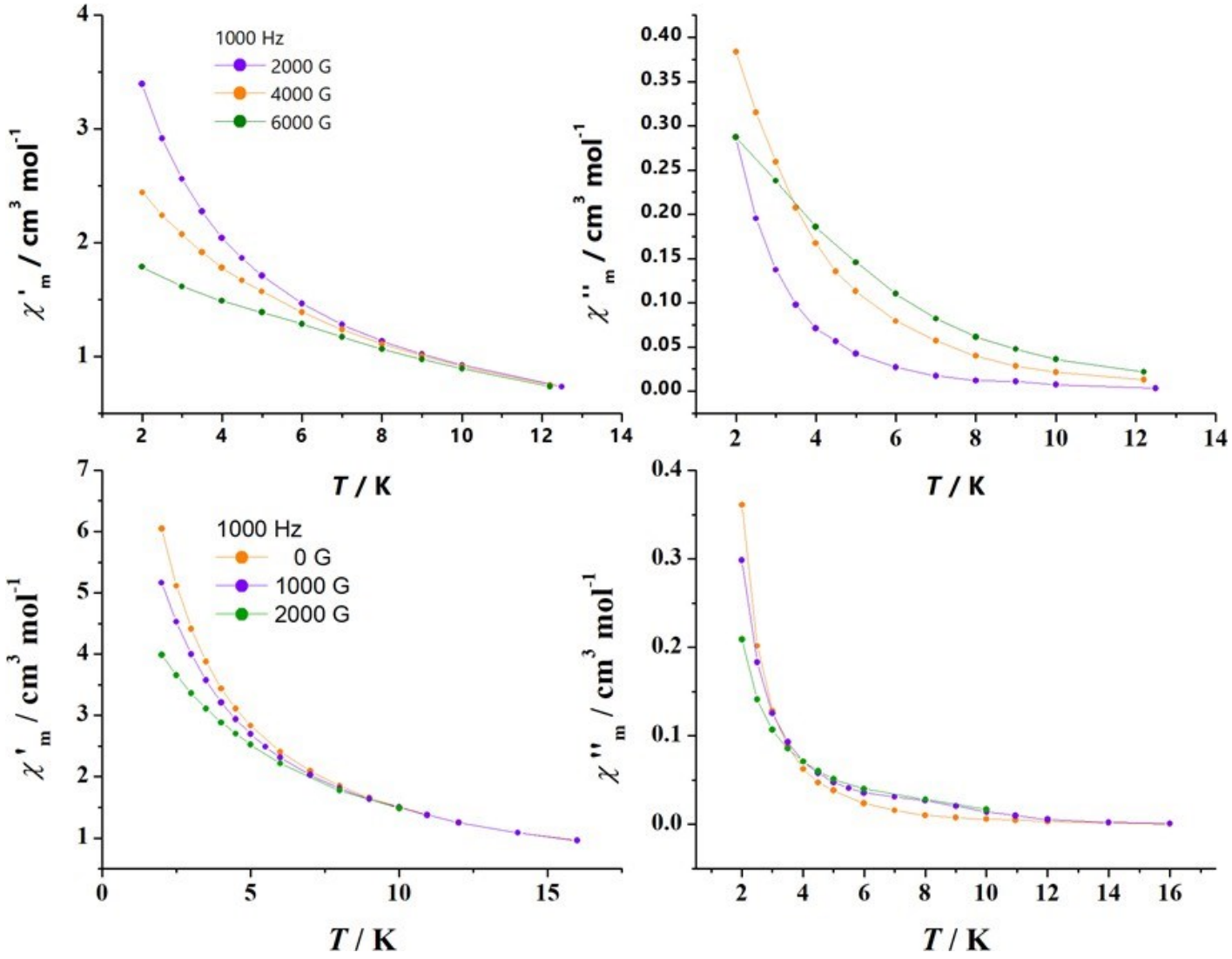

Fig. S15 Ac plots under various external fields, at a constant frequency of 1000 Hz, for complexes **5** (top) and **7** (bottom).

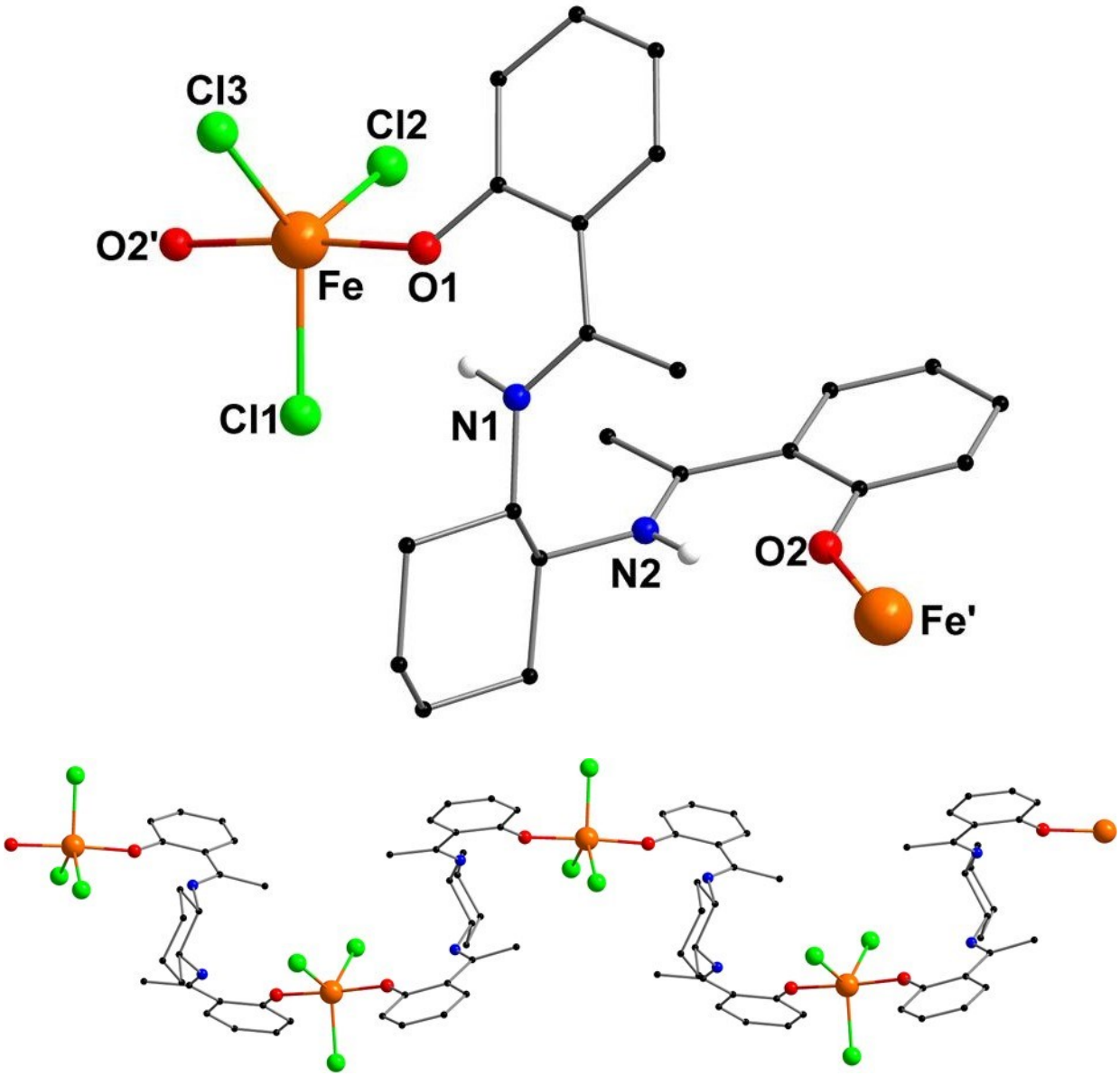

Fig. S16 (Top) The asymmetric unit and (bottom) a small portion of the 1-D chain of $\{[Fe^{III}Cl_3(LH_2)]\cdot Et_2O\}_n$.

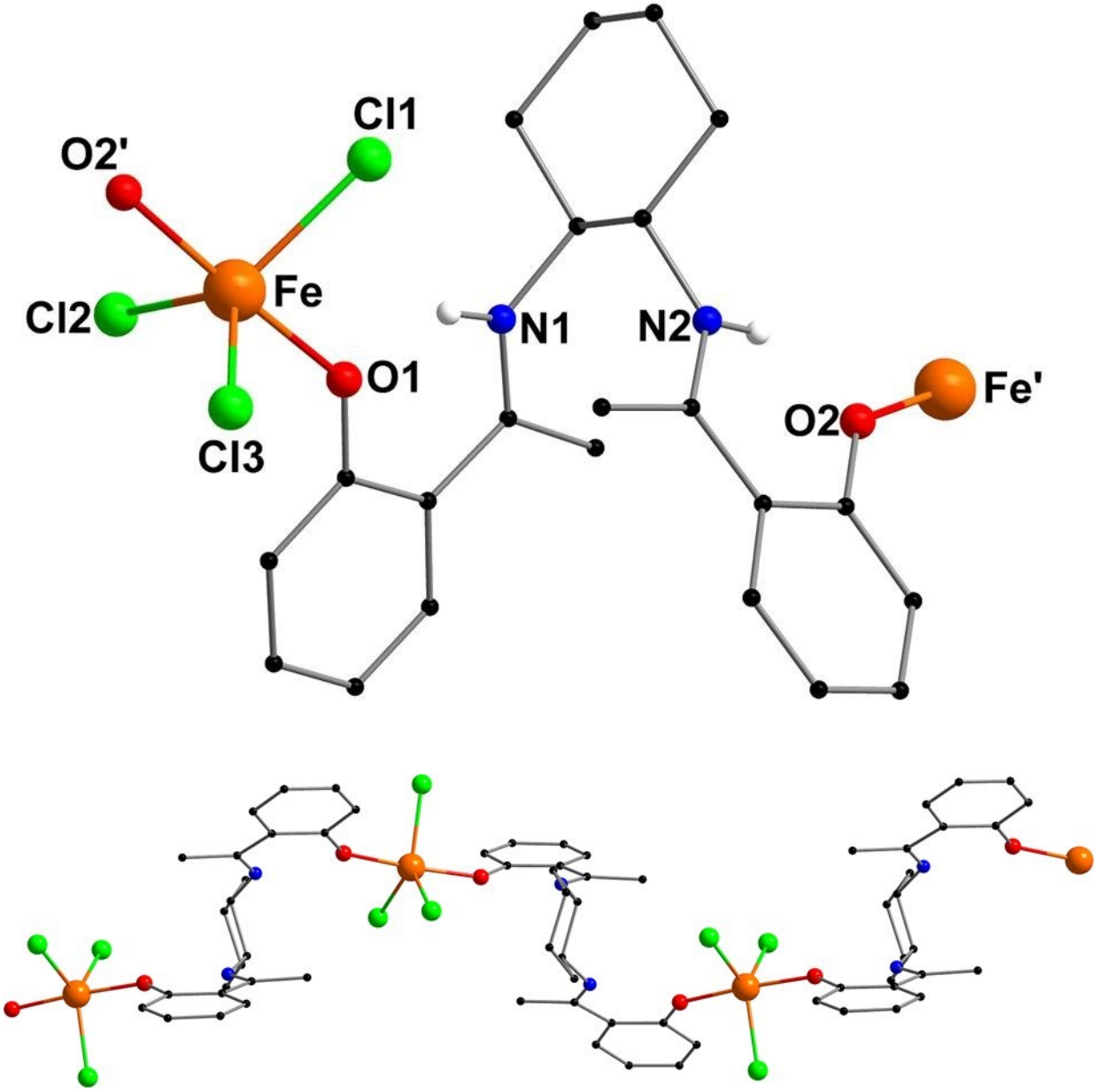

Fig. S17 (Top) The asymmetric unit and (bottom) a small portion of the 1-D chain of $\{[Fe^{III}Cl_3(LH_2)]\cdot 2Me_2CO\}_n$.

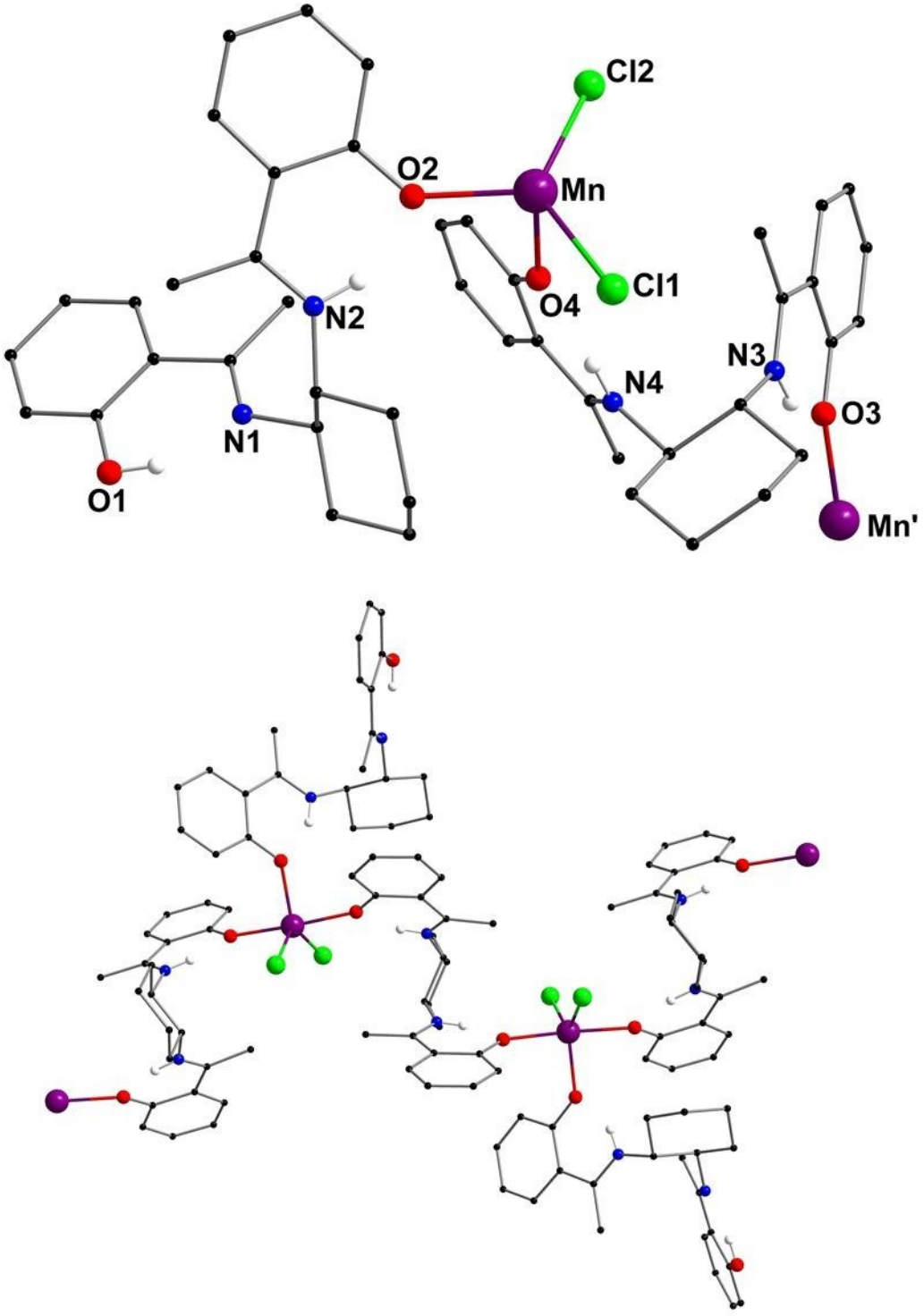

Fig. S18 (Top) The asymmetric unit and (bottom) a small portion of the 1-D chain of $\{[Mn^{II}Cl_2(LH_2)_2]\cdot 3MeOH\}_n$.

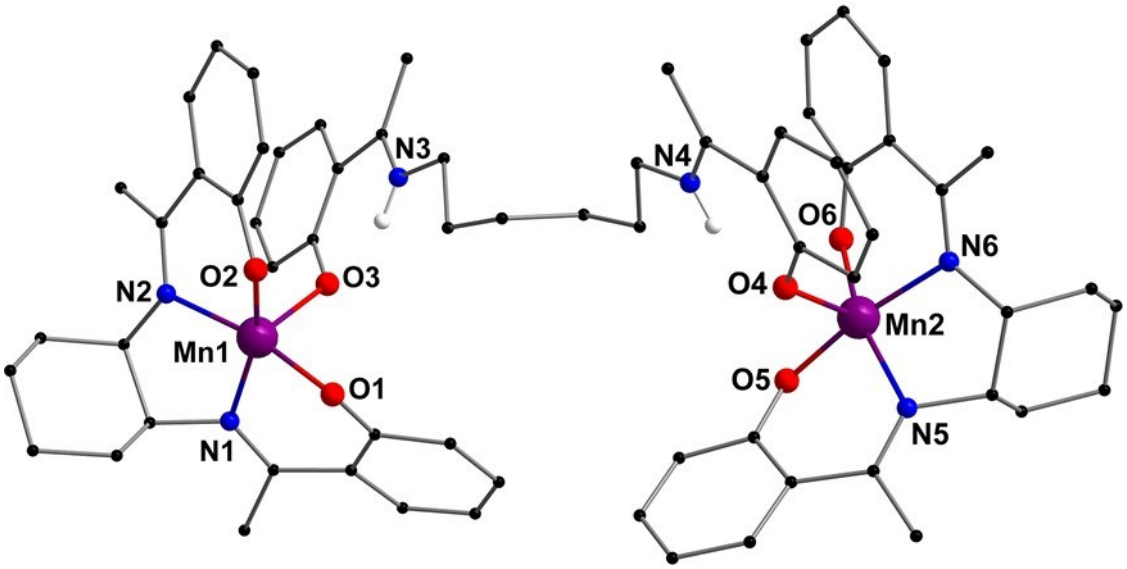

Fig. S19 Structure of the dinuclear anion that is present in the crystal structure of $(Et_3NH)[Mn^{III}_2(L)_2(L'H_2)](ClO_4)_3 \cdot CHCl_3$; the anion contains both the doubly deprotonated form (L^{2-}) of the initially used ligand LH_2 and the neutral bridging transformed ligand $L'H_2$.

Mechanistic discussion and proposals

The Ln^{III}-assisted LH_2 => $L'H_2$ transformation, observed in this work, was totally unexpected. Ring opening of cyclohexane to form *n*-hexane (hydrogenolysis of one C-C bond) requires noble metal-containing catalysts supported on various oxide substrates (*e.g.* Al_2O_3, SiO_2, WO_3/ZrO_2, …) and harsh conditions (temperatures > 200 °C and high H_2 pressures).[1] When we observed the Ln^{III}-assisted LH_2 => $L'H_2$ transformation in **1**-**11**, our first though was that the obvious H_2 source was MeOH, one of the solvents used for the preparation of **1**-**11**. MeOH is a promising hydrogen source and could be the base for a future economy, owing to its low cost, bioreproducibility and high H_2 content (12.5 wt %). However, the dehydrogenation of MeOH is energetically demanding (~ 64 kJ mol^{-1}) and it thus requires high temperatures, while there is a high probability for CO formation.[2] Organometallic Rh^{III} [1a] and Ir^{III} [1b] catalysts have been recently found to show excellent activity in dehydrogenation of MeOH at room temperature, the substrates being aldehydes and α,β-unsaturated ketones. In a very recent report, [2c] the catalytic utilization of MeOH as a H_2 source for the reduction of different organic compounds, such as nitroarenes, olefins and carbonyl compounds, was described. The key to success of these transformations is the use of a commercially available Pt/C catalyst, which enables the transfer hydrogenation of nitroarenes-to-anilines, alkenes-to-alkanes and aldehydes-to-alcohols using MeOH as both the solvent and H_2 donor; the reactions were performed at 150 °C.

The above mentioned experimental literature led us to propose, in the originally submitted ms, the mechanism shown in Scheme S1 (Scheme 3 of the originally submitted ms), with an alternative representation of the transformation of LH_2 to intermediate **II** being illustrated in Scheme S2 (Scheme 4 of the originally submitted ms).

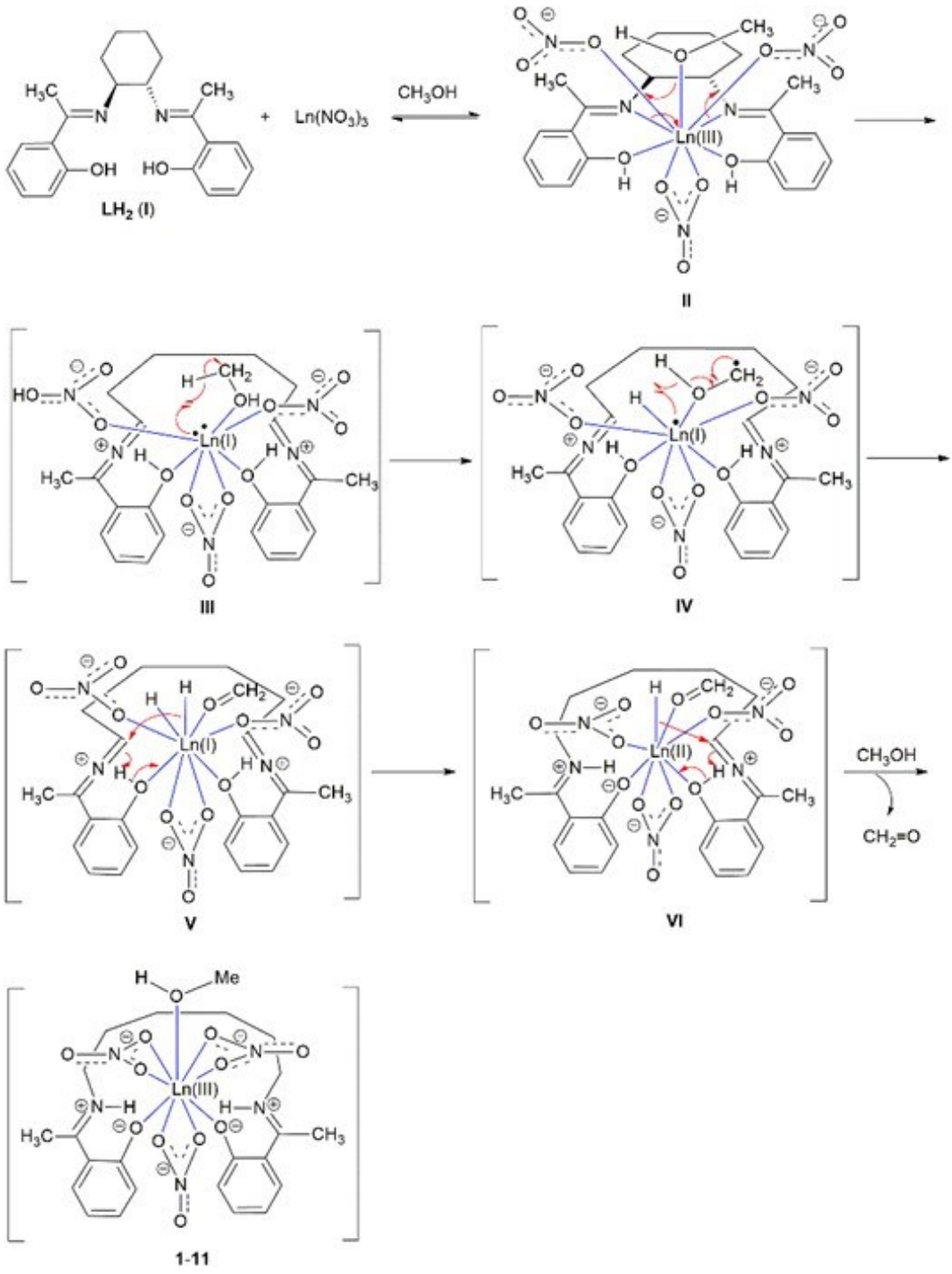

Scheme S1 Originally proposed mechanism for the Ln^{III}-assisted $LH_2 \rightarrow L'H_2$ transformation and formation of the final products **1**-**11**. To avoid congestion, only one of the nitrato groups has been drawn as bidentate chelating in the intermediates **II**-**VI**. The three nitrato ligands are chelating in the final products (**1**-**11**) and most probably also in the intermediates **II**-**VI**.

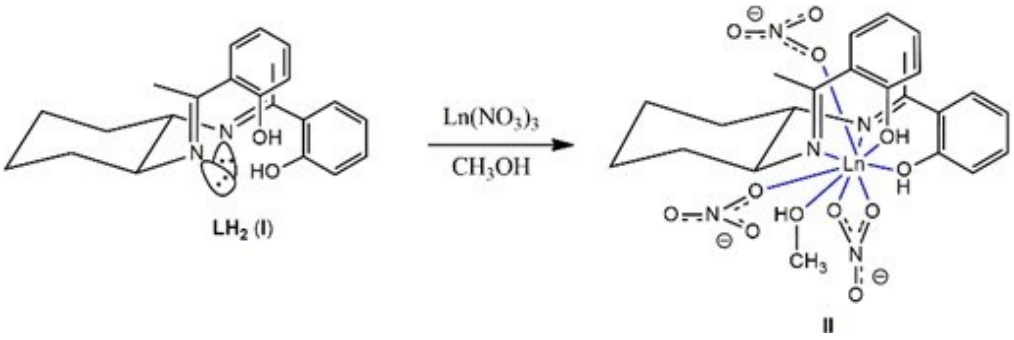

Scheme S2 Originally proposed, alternative formation of the intermediate complex **II** from the reaction of the original Schiff base LH_2(**I**) and lanthanoid(III) nitrates in MeOH. To avoid congestion, only one of the nitrato groups has been drawn as bidentate chelating.

Of course we were aware that the most perculiar feature of the originally proposed ms (Scheme S1) concerns the low oxidation states (I, II) of the *transient lanthanoid species* . It is well known[3] that the common oxidation state for the lanthanoids is III, but the IV one is also known for Ce, Pr, Nd, Tb and Dy. Relatively recent theoretical and experimental studies have verified the existence of Pr(V) species.[4] The oxidation state II has been found for all lanthanoids,[5] albeit in organometallic compounds. Evidence for the existence of Ln(I) species had been reported, [6a-f] but proof of this was lacking. However, performing a combined photoelectron spectroscopy and quantum theoretical study, a Chinese group[6g,h] showed that the I oxidation state can be stabilized in the boride-cluster species $[(Ln^{I}(B_4^{2-})]^{-}$ and in borazene complexes of the type $[(Ln^{I}(B_8^{2-})]^{-}$; these studies proved the existence of the Ln(I) complexes, impressively expanding the chemistry of the 4f metals.

Due to the fact that transient Ln(I) species (Scheme S1) might be highly improbable, we devised the mechanism shown in Scheme S3 below, which was <u>not</u> included in the originally submitted ms. The mechanism (which is essentially similar with that presented in Scheme S1) does not propose Ln(I) species, but only Ln(II).

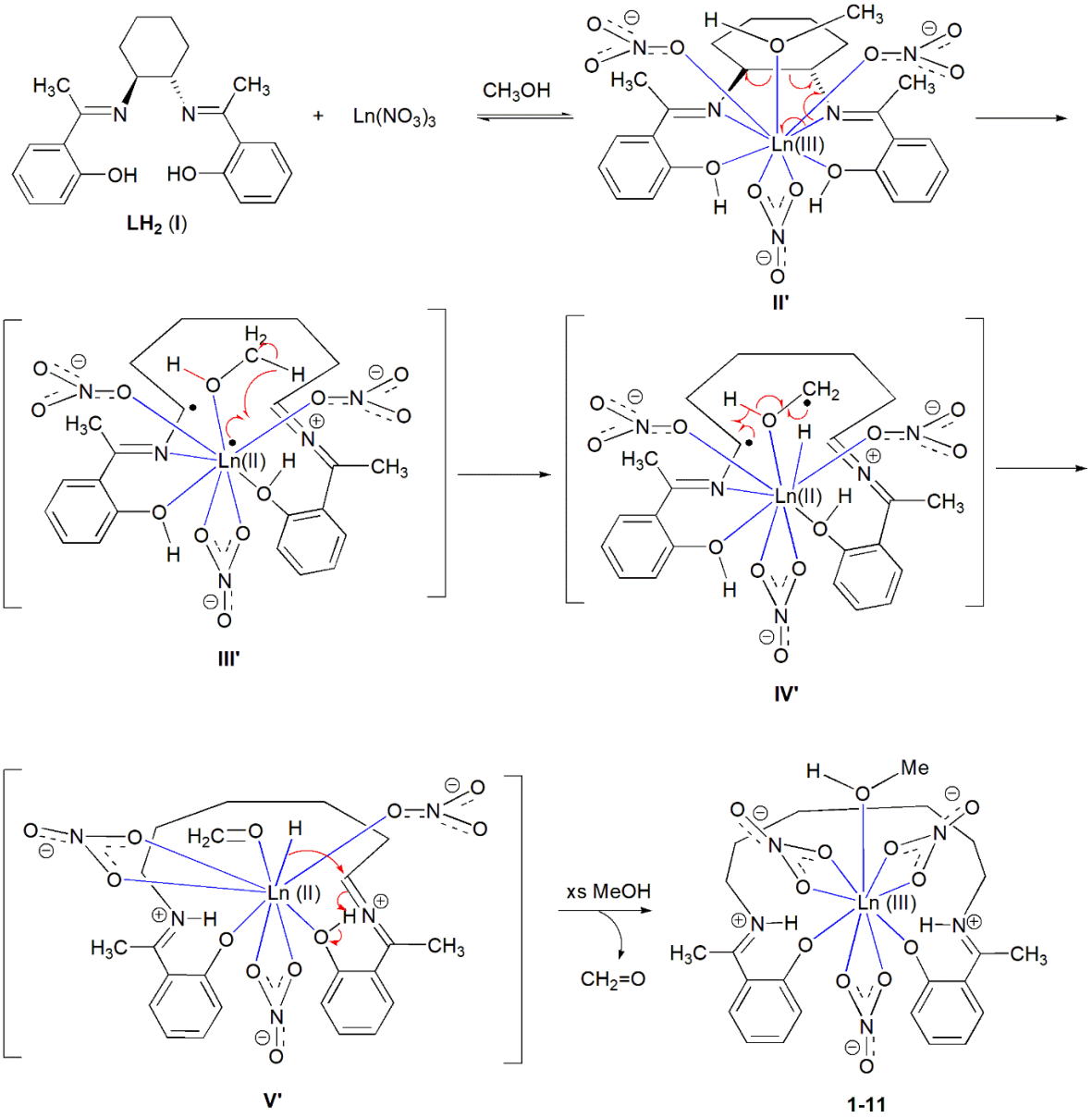

Scheme S3 An alternative, to that presented in Scheme S1, mechanism for the Ln^{III}-assisted LH_2 => $L'H_2$ transformation and formation of the final products **1**-**11**. This proposal does not involve 2-electron reduction lanthanoid species, but only 1-electron reduction lanthanoid species ; however, this mechanistic proposal does assume (as in Scheme S1) that MeOH is the H_2 source. To avoid congestion and/or retain the coordination number at the Ln^{III} atom 8 or 9, only one (in **II'**-**IV'**) and two (in **V'**) nitrato groups have been drawn as bidentate chelating. The three nitrato groups are chelating in the final products and probably in some intermediates.

However it turned out that the mechanisms presented in Schemes S1-S3 can not be correct. Following the valuable suggestions by Referee 1, [7] we performed the 1:2 reaction of

$Y(NO_3)_3{\cdot}6H_2O$ (in order to use ^1H NMR spectroscopy for the characterization of the product(s)) and LH_2 in other solvents *i.e.* MeCN or Me_2CO/CH_2Cl_2. Somewhat to our surprise, the obtained solid **11a (**the same in both solvent media) was very similar with product **11**, the only difference being the replacement of the MeOH ligand in the latter by an aqua ligand in the former (analytical, IR and ^1H NMR evidences), please see "Synthetic procedures" in the "Experimental section" of the revised main text. *This proves that MeOH is not the H_2 source in the LnI^{II}-assisted transformation LH_2 => $L'H_2$.*

Also, following Referee's 1 suggestion: (a) We obtained immediately the same products (in the form of crystalline powders) employing concentrated solutions of the reactants, possibly indicating that the transformation proceeds into the solution and is not a result of the crystallization process ; and (b) We re-examined carefully the 1:1 reactions and found negligible yields of the products.

In order to further confirm the non-involvement of MeOH in the mechanism of the transformation, we also isolated product $[Y(NO_3)_3(L'H_2)(CD_3OD)]$ (**11b**), see "Synthetic procedures" in the "Experimental section" of the revided main text. Its ^1H NMR spectrum in d_6-DMSO is almost identical with that of **11**. Again the intergrations of the δ 3.58, 1.64 and 1.50-1.30 ppm signals, due to the $-(CH_2)_6-$ protons, is 1:1:1 (or 4:4:4). If MeOH was involved in the mechanism (Schemes S1 and S3), the methylene groups attached to N atoms in the deuterated product would have been –CHD- (and not $N(CH_2)$) and the intergration ratio would have been 2:4:4. In other words, if MeOH is the H_2 source, two of its H atoms should be expected to be incorporated into the final products, and in particular into the methylene groups next to the N atoms and thus D atoms should be found in the deuteriated complex.

All the above experimental facts, clearly point out a mechanism where a second LH_2 molecule is the source of H_2. Our mechanistic proposal is illustrated in Scheme S4.

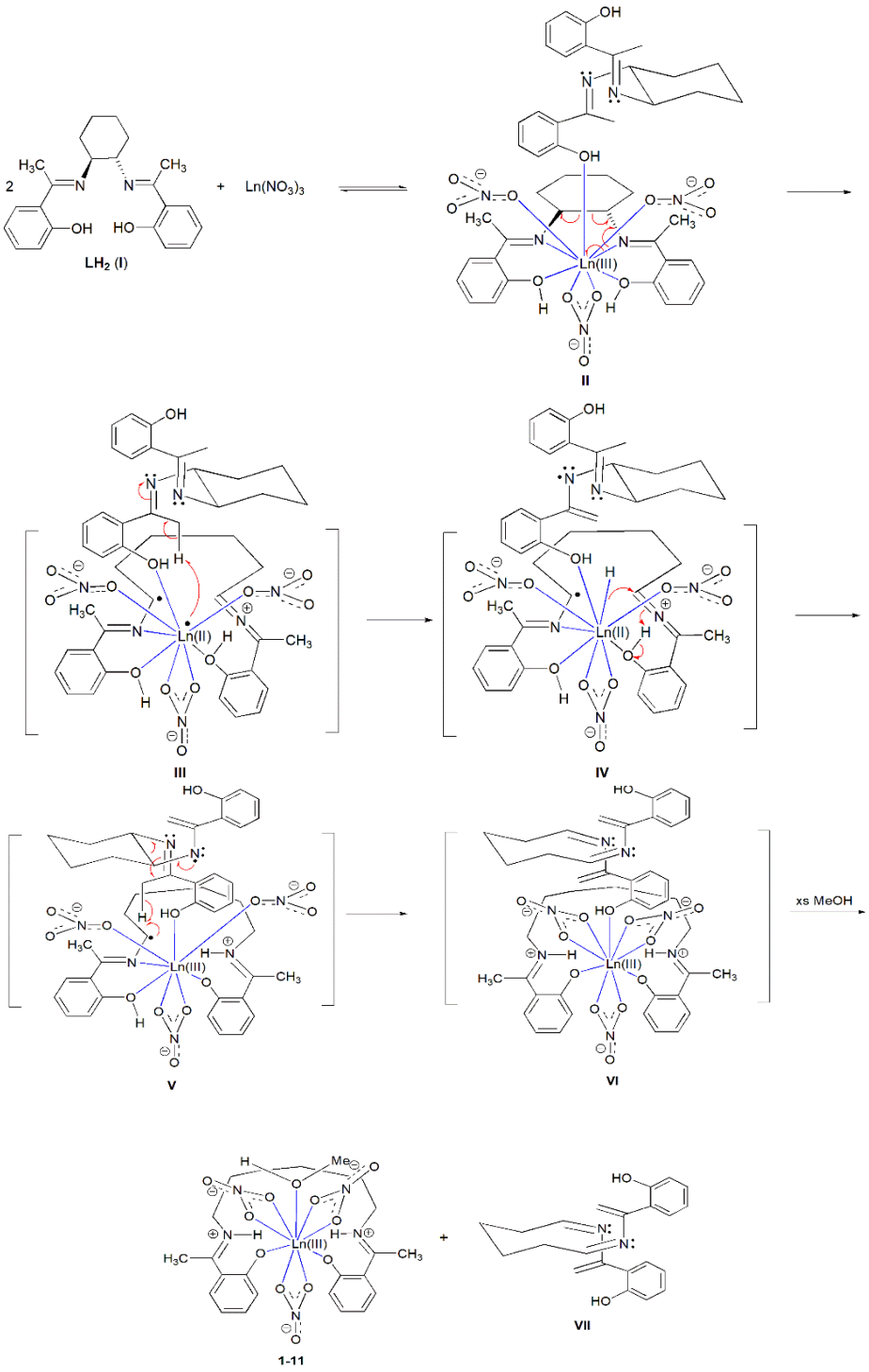

Scheme S4 Proposed mechanism for the Ln^{III}-assisted LH_2 => $L'H_2$ transformation and formation of **1**-**11**. To avoid congestion and/or retain the coordination number at the Ln^{III} atom 8 or 9, only one of the three nitrato groups has been drawn as bidentate chelating ligand in the intermediates **II**-**V**. Note that all three nitrato groups are bidentate chelating in the final products (**1**-**11).**

Thus, the reaction of the LH_2(**I**) with $Ln(NO_3)_3 \cdot xH_2O$ (x= 5 or 6) in the 2:1 ratio to form complexes **1**-**11** through cyclohexyl C-C bond cleavage is proposed to take place as follows, taking into consideration the crucial role of the two -CH_3 groups on the ligand. The methyl groups are not present in the corresponding ligand salcnH_2 (Scheme 1 of the originally submitted and revised ms), which upon reaction with lanthanoid (III) ions provide complexes in which the ligand remains always intact.[8] Initial formation of **II** between two molecules of LH_2, one acting as tetradentate ligand and the other as monodentate ligand (such coordination behaviours have been observed in Ln^{III} complexes od salcnH_2 [8d,h]) and the $Ln(NO_3)_3$ unit, followed by an one-electron oxidative glycol cleavage-type of the cyclohexyl C-C bond,[9,10] leads to the new complex **III** with Ln^{III} => Ln^{II} reduction and the simultaneous creation of an allylic-type secondary C-centered free radical. An alternative representation of LH_2 (**I**) to **II** is shown in Scheme S5. Complex **II** is crowded and therefore the driving force behind the subsequent C-C bond cleavage is probably the release of steric strain. The next step involves transfer of an allylic-type H atom from the –CH_3 group to Ln^{II} leading to the Ln^{II} hydride complex **IV** and a N-centered free radical. Reduction of the bisiminium functionality with the adjacent double bonds by the hydride converts intermediate **IV** to the biradical intermediate **V**. The C-centered free radical is then reduced by a second H atom transfer from the –CH_3 group of the monodentate ligand in the way depicted in Scheme S4 to give the new intermediate **VI**. Excess MeOH, used as co-solvent in the reaction, displaces then the monodentate ligand to provide the final complexes **1**-**11**.

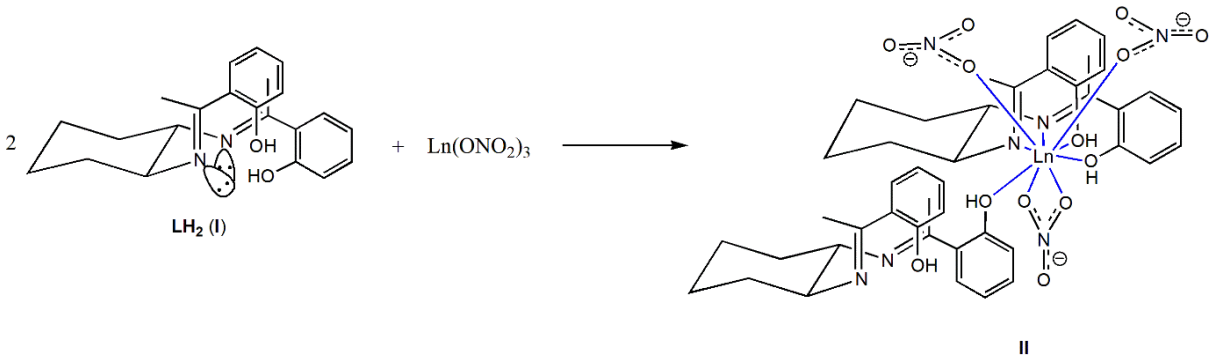

Scheme S5 Formation of the intermediate complex **II** (see Scheme S4) from the 2:1 reaction between LH_2 and lanthanoid(III) nitrates. To avoid congestion and/or retain the coordination number at the Ln^{III} centre 9, only one of the three nitrato groups has been drawn as bidentate chelating ligand.

Alternatively, the conversion of the intermediate **V** to intermediate **VI** can be envisaged to take place through the mediation of the metal centre as depicted in Scheme S6.

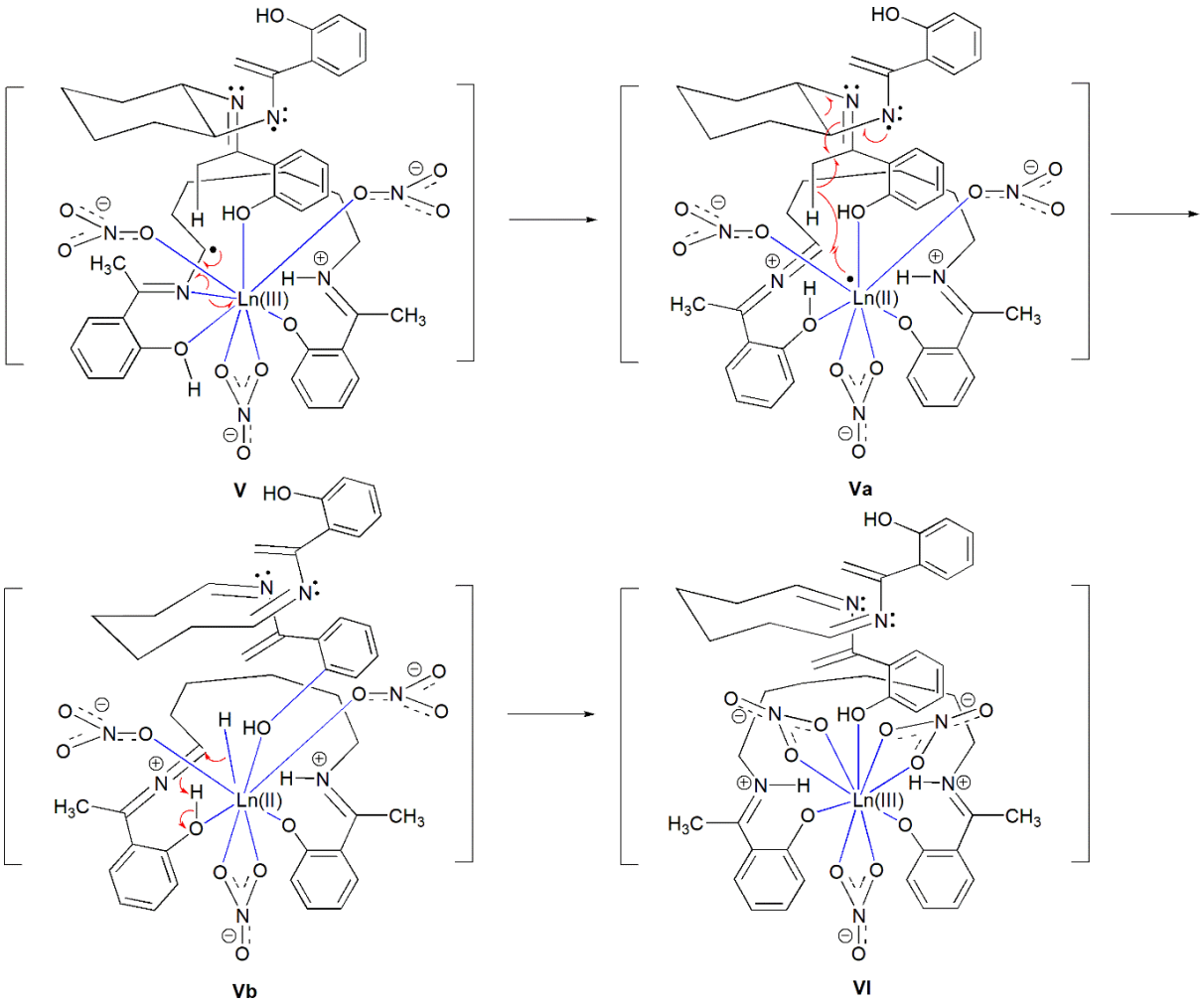

Scheme S6 Alternative steps for the conversion of intermediate **V** *en route* to the formation of complexes **1**-**11**.

Two further mechanistic points deserve discussion. First, the 1:2 reaction between $Y(NO_3)_3 \cdot 6H_2O$ and LH_2 in MeOH-CH_2Cl_2 *under a nitrogen atmosphere* (albeit with solvents used as received commercially) led again to complex **11** (IR evidence), suggesting that atmospheric oxygen is not involved in the mechanism (this point was raised by Referee 2 [7]). Second, the nitrate could be the primary oxidant (and not Ln^{III}) in the process.[11,12] In such a case, the nitrite produced in the reaction would be reoxidized to nitrate by O_2 in the presence of Ln^{III}. Such a possibility can be excluded in our case. The 1:2 reaction between $YCl_3 \cdot 6H_2O$ (*i.e.* a non-nitrate starting material) and LH_2 in MeOH-CH_2Cl_2 gave a solid satisfactorily analyzed as

$[YCl_3(L'H_2)(MeOH)_y]$ (y = 3 or 4) ; its ^1H NMR spectrum in d_6-DMSO is identical with that of the nitrato complex **11**. This shows that the nitrates are not essential for the transformation.

Theoretical discussion in brief

A first theoretical approach for the ligand transformation has been attempted with the goal to understand the great thermodynamic stability of $[Pr(NO_3)_3(L'H_2)(MeOH)]$ (**1**), and hence that of the other complexes (**2**-**12**). The structures of the obtained complex **1** (in which the ligand has been transformed) and the hypothetical complex $[Pr(NO_3)_3(LH_2)(MeOH)]$ (**1'**) were computationally found and shown in Scheme S7. Complex **1'** consists of a 9-coordinate Pr^{III} atom, with one coordinated molecule of MeOH, three bidentate chelating nitrato groups and one O, O'-bidentate chelating bis(zwitterionic) molecule of the initially used LH_2 compound as ligand ; it is thus structurally similar with **1**.

It is worth mentioning at this point more specifically the changes observed during the reaction, but also the way in which they should be simulated. The cyclohexyl ring was broken, and it turned into an open carbon chain at the ends of which two more H atoms were added. Therefore, a reasonable simulation of the observed transformation would be the conversion of an 1,2-diaminocyclohexane to an 1,6-diaminohexane model molecule, as shown in Scheme S8. The energy difference (ΔG) between these two model molecules should be added to the energy of the hypothetical complex **1'**, before comparing it with that of the prepared (obtained) complex **1**.

As can be easily seen in Scheme S7, the prepared complex **1** (a) exhibits an extended structure in space (due to the cleavage of the cyclohexyl ring and the creation of the corresponding open $-(CH_2)_6-$ chain) by contrast with the hypothetical **1'** (b) which exhibits a more compact structure. This reduces the intramolecular repulsions in the former, increasing them in the latter. This, in turn, could lead to a better thermodynamic stabilization of **1** than of **1'** ; the corresponding energy difference (ΔG) was calculated to be 26.8 kcal/mol.

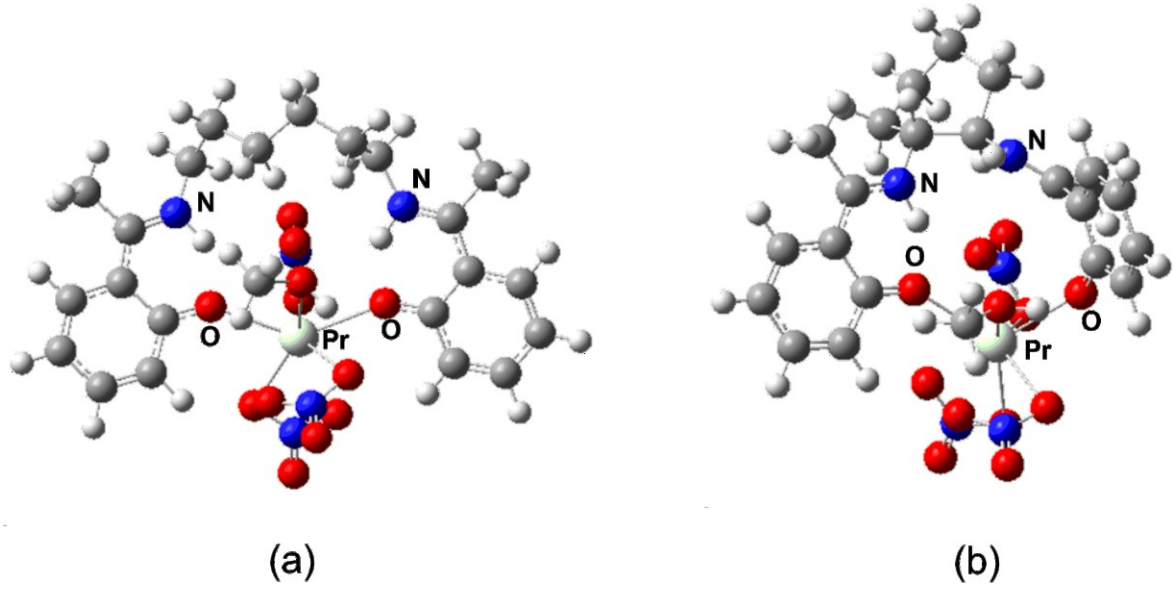

Scheme S7 Gas-phase calculated structures of the prepared complex **1** (a) and the hypothetical complex **1'** (b). Symbols of a few atoms are only given for clarity, such as i) the two adjacent N atoms attached to the cyclohexane ring in **b**, which are significantly removed by ring opening in **a**, and ii) the O atoms of the organic ligands coordinated to Pr^{III}.

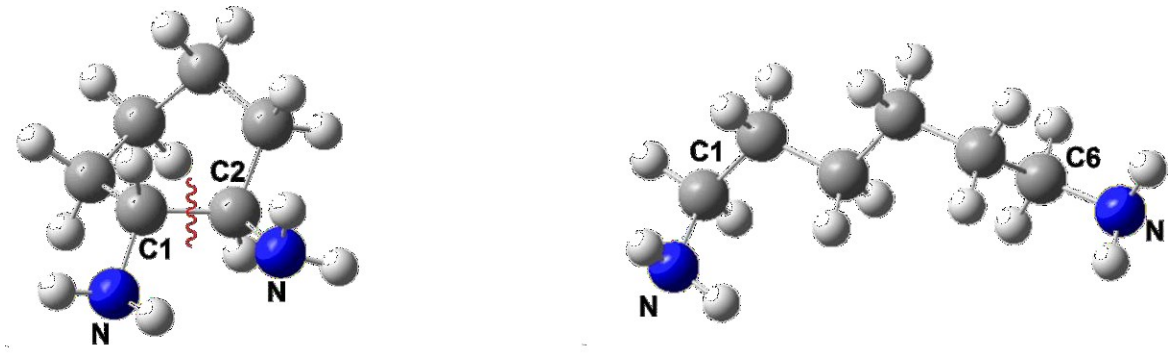

Scheme S8 The computational structures of the model molecules 1,2-diaminocyclohexane (left) and 1,6-diaminohexane.

References for the ESI

1. *(a)* Y. Miki, S. Yamadaya and M. Oba, *J. Catal.*, 1977, **49**, 278-284; *(b)* L.M. Kustov, T.V. Vasina, O.V. Masloboishchikova, E.G. Khelkovskaya-Sergeeva and P. Zeuthen, *Stud. Surf. Sci. Catal.*, 2000, **130**, 227-232; *(c)* O.V. Masloboishchikova, T.V. Vasina, E.G. Khelkovskaya-Sergeeva, L.M. Kustov and P. Zeuthen, *Russ. Chem. Bull., Intern. Edit.*, 2002, **51**, 249-254; *(d)* T.V. Vasina, O.V. Masloboishchikova, E.G. Khelkovskaya-Sergeeva, L.M. Kustov and P. Zeuthen, *Russ. Chem. Bull., Intern. Edit.*, 2002, **51**, 255-258.

2. *(a)* Z. Chen, G. Chen, A.H. Aboo, J. Iggo and J. Xiao, *Asian J. Org. Chem.*, 2020, **9**, 1174.; *(b)* N. Garg, H.P. Somasundharam, P. Dahiya and B. Sundararaju, *Chem. Commun.*, 2022, **58**, 9930-9933; *(c)* V. Goval, T. Bhatt, C. Dewangan, A. Narani, G. Naik, E. Baharaman, K. Natte and R.V. Jagadeesh, *J. Org. Chem*., 2023, **88**, 2245–2259.

3. H.C. Aspinall, *f-Block Chemistry*, Oxford University Press, Oxford, UK, 2020, pp. 13-14, 28-32.

4. *(a)* S.-X. Hu, J. Jian, J. Su, X. Wu, J. Li and M. Zhou, *Chem. Sci.*, 2017, **8**, 4035-4043; *(b)* Q. Zhang, S.-X. Hu, H. Qu, J. Su, G. Wang, J.-B. Lu, M. Chen, M. Zhou and J. Li, *Angew. Chem., Int. Ed.*, 2016, **55**, 6896-6900.

5. For example, see: *(a)* W.J. Evans, *Inorg. Chem.*, 2007, **46**, 3435-3449; *(b)* A.J. Ryan, L.E. Darago, S.G. Balasubramani, G.P. Chen, J.W. Ziller, F. Furche, J.R. Long and W.J. Evans, *Chem.- Eur. J.*, 2018, **24**, 7702-7709; *(c)* G. Meyer, *Angew. Chem., Int. Ed.*, 2014, **53** 3550-3551; *(d)* M.N. Bochkarev, *Coord. Chem. Rev.*, 2004, **248**, 835-851; *(e)* P.B. Hitchcock, M.F. Lappert, L. Maron and A.V. Protchenko, *Angew. Chem.*, *Int. Ed.,* 2008, 1488-1491.

6. *(a)* F.K. Fong, J.A. Cape and E.Y. Wong, *Phys. Rev.*, 1966, **151**, 299-303; *(b)* F.K. Fong, J.B. Fenn, Jr. and J.O. McCaldin, *J. Chem. Phys.*, 1970, **53**, 1559-1565; *(c)* G. Schoendorff and A.K. Wilson, *J. Chem. Phys.*, 2014, **140**, article 224314; *(d)* R.S. Ram and P.F. Bernath, *J. Chem. Phys.*, 1996, **104**, 6444-6451; *(e)* X. Cao,

W. Liu and D. Michael, *Sci. China, Ser. B*, 2002, **45**, 91-96; *(f)* J. Zhang, G. Pagano, P.W. Hess, A. Kyprianidis, P. Becker, H. Kaplan, A.V. Gorshkov, Z.X. Gong and C. Monroe, *Nature*, 2017, **551**, 601-609; *(g)* X. Chen, T.-T. Chen, W.-L. Li, J.-B. Lu, L.-J. Zhao, T. Jian, H.-S. Hu, L.-S. Wang and J. Li, *Inorg. Chem.*, 2019, **58**, 411-418.

7. We thank the referees for their valuable revision ponits/comments/suggestions.

8. *(a)* G.-L. Wang, Y.-M. Tian, D.-X. Cao, Y.-S. Yu and W.-B. Sun, *Z. Anorg. Allg. Chem.*, 2011, **637**, 583-588; *(b)* G.-L. Wang, Y.-M. Tian, W.-B. Sun, B.-L. Han, M.-F. Yu, H. Xu and T. Gao, *Z. Anorg. Allg. Chem.*, 2011, **637**, 1616-1621; *(c)* J. Zhu, H.-F. Song, P.-F. Yan, G.-F. Hou and G.-M. Li, *Cryst. Eng. Commun.*, 2013, **15**, 1747-1752; *(d)* Q. Liu, M. Ding, Y. Lin and Y. Xing, *Polyhedron*, 1998, **17**, 555-559; *(e)* Q. Liu and M. Ding, *J. Organomet. Chem.*, 1998, **553**, 179-181; *(f)* Q. Liu, J. Huang, Y. Qian and A.S.C. Chan, *Polyhedron*, 1999, **18**, 2345-2350; *(g)* J. Zhu, H. Song, J. Sun, P. Yan, G. Hou and G. Li, *Synth. Metals*, 2014, **192**, 29-36; *(h)* P.-F. Yan, P.-H. Lin, F. Habib, T. Aharen, M. Murugesu, Z.-P. Deng, G.-M. Li and W.-B. Sun, *Inorg. Chem.*, 2011, **50**, 7059-7065; *(i)* J.-W. Sun, J. Zhu, H.-F. Song, G.-M. Li, X. Yao and P.-F. Yan, *Cryst. Growth Des.*, 2014, **14**, 5356-5360; *(j)* X. Zou, C. Du, Y. Dong and G. Li, *Inorg. Chim. Acta*, 2020, **507**, article 119455.

9. W. S. Trahanovsky, L. H. Young and M.H.Bierman, *J. Org. Chem.,* 1969, **34**, 869-871.

10. J. March, *Advanced Organic Chemistry*, Wiley, New York, USA, 4th edn, 1992, pp. 1174-1177.

11. G. A. Molander, *Chem. Rev.*, 1992, **92**, 29-68.

12. P. Girard and H. B. Kagan, *Tetrahedron Lett.*, 1975, 4513-4515.

Author contributions

I.M.-M.: conceptualization, synthesis and data analysis; Z.L.: Raman spectroscopy and data analysis; A.K.: synthesis and conventional characterization; D.M.: synthesis and conventional characterization; K. Skordi: collection of single-crystal crystallographic data; A.T.: supervision of the experimental work on single-crystal crystallography; V.B.: luminescence spectra and data analysis; A.E.: supervision of the experimental magnetic work; J.M. magnetic measurements, data analysis and writing the magnetic part of the manuscript; V.N.: solution and refinement of the single-crystal X-ray structures and creation of structural plots; E.B.: theoretical calculations and writing the relevant part of the manuscript; D.P.: mechanistic proposals and writing the relevant part of the manuscript; and S.P.: conceptualization, supervision, project management, and final manuscript writing and editing.